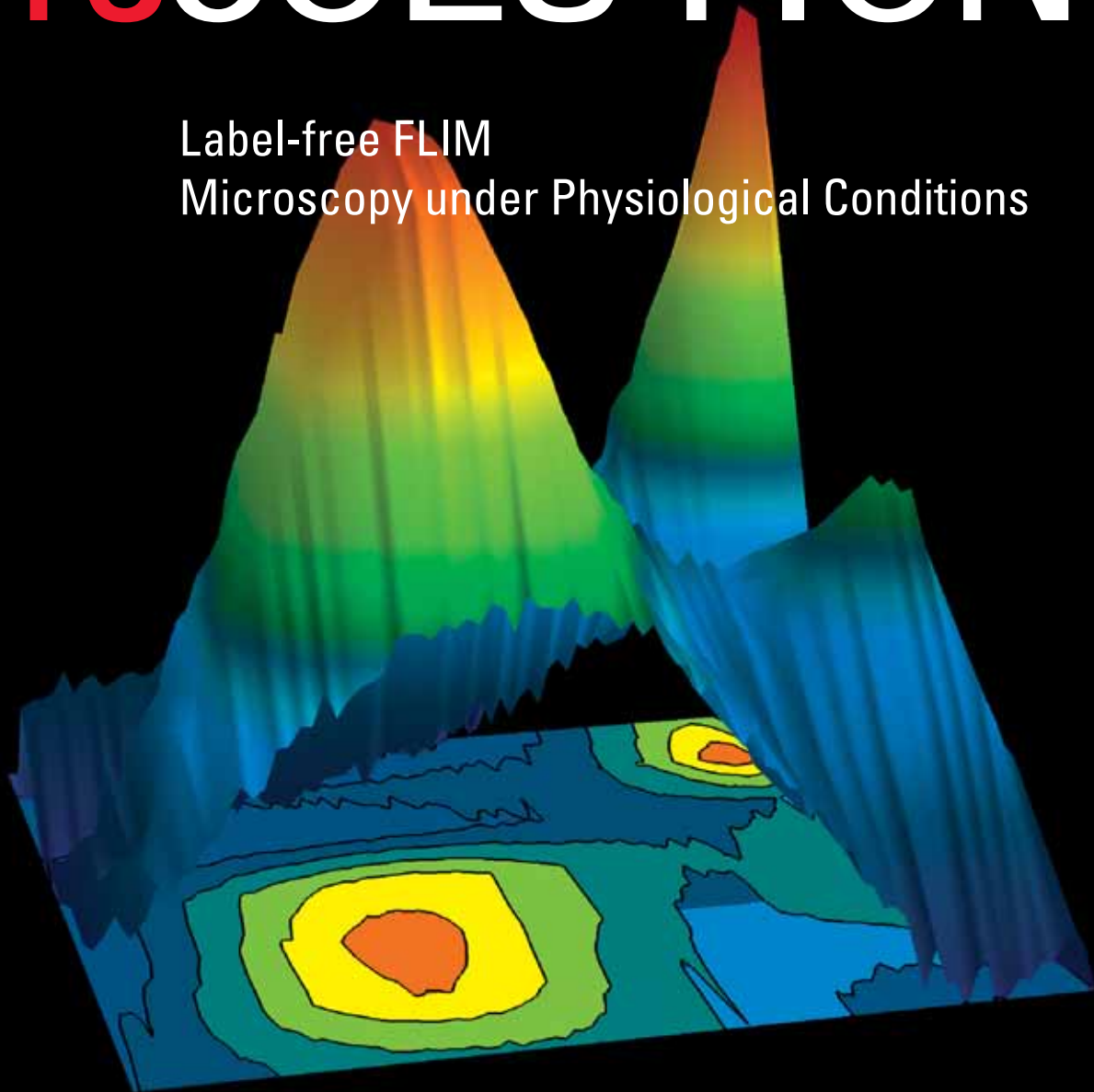


June  
2009  
No. 34

CONFOCAL APPLICATION LETTER

# reSOLUTION

Label-free FLIM  
Microscopy under Physiological Conditions



## Abstract

Many biological samples exhibit autofluorescence. Its often broad spectra can interfere with fluorescent labeling strategies. This application letter demonstrates how autofluorescence can serve as an intrinsic contrast in fluorescence lifetime imaging microscopy (FLIM) resulting in multi-color image stacks. It is also outlined how to combine spectral imaging with fluorescence lifetime information to distinguish and potentially identify different fluorescent species in biological samples.

## Microscopy meets autofluorescence

In fluorescence microscopy generally autofluorescence is viewed as a detrimental side-effect inherent to many biological samples. It tends to overlap with endogenous fluorescence labels sometimes masking its intensity. It can cause difficulties with spectral channel separation and with quantitation of intensities for ratiometric analysis. The often very broad emission spectra of autofluorescence can render it intractable by conventional spectral image recording.

However, autofluorescence as such has its merits, too. It is an intrinsic form of fluorescent label which comes for free and is completely non-invasive. The purpose of this application letter is

to identify several autofluorescent components by means of fluorescence lifetime imaging microscopy (FLIM) and to demonstrate their utility in biomedical research.

**Note:** For a basic treatment of the FLIM technique please refer to the application letter FLIM-FRET (number 35).

## Autofluorescence meets science

Most biological samples contain biochemical species which can give rise to autofluorescence. For example a cell's redox potential is reflected in its concentration of NAD(P)H and flavins. The former are better excited with IR sources, the latter are accessible with 405 nm as well. Quite a few structural proteins can deliver lifetime contrast as well, such as collagen, elastin and fibrillin.

Plant cells are particularly rich in a multitude of autofluorescent molecules. Very common are chlorophyll, carotenoids, polyphenols to name but a few. Often, these compounds can not only provide label-free contrast, but also provide information on the metabolic state or pathogenic alterations in cells or tissues. Thus, one can draw functional conclusions by combining FLIM and autofluorescence.

## Cover picture:

2D lifetime – wavelength spectrum.

Sum of three autofluorescent components.

### Label-free contrast

To exemplify the utility of autofluorescence as a contrasting strategy in biological samples we shall examine an example from the animal and the plant kingdom, respectively.

Let us begin with a scale insect. Different developmental stages of this plant parasite were collected and immediately mounted. An overview image of the autofluorescence present at the excitation wavelength 470 nm was recorded using a 10x objective (Fig. 1). The intensity image was created from a FLIM data set and yields a good representation of the structure of the specimen. Intensity here encodes counted photons per pixel instead of arbitrary units as customary for standard intensity images. It is, however, unable to distinguish any autofluorescent species (Fig. 1 A). This information is contained in the lifetime map (Fig. 1 B) which renders the spatially resolved lifetime distribution. It gives a good impression of the different fluorescent lifetime components. In terms of autofluorescence this

often represents different molecular species or combinations thereof. We can distinguish very well the chitinized exoskeleton around the antennae and the legs (green to blue). Chitin displays a very short lifetime. The surrounding tissue appears relatively homogenous close to 3 ns (yellow). Some interspersed regions with longer lifetimes (orange) could represent other species, but here, they more likely represent darker regions which simply have a lower precision in determining the lifetime. What is typically perceived and communicated as a FLIM image is in fact an intensity modulated lifetime map (Fig. 1 C). The lifetime information is multiplied by the intensity image. This rendition tends to de-emphasize the darker regions with poor photon statistics and it retains more of the structural information contained in the intensity image. The latter often facilitates the interpretation of lifetimes as in the case of the orange regions in the lifetime map. We can conclude that FLIM allows us to identify different molecular species in an unperturbed sample and to study their spatial interrelation.

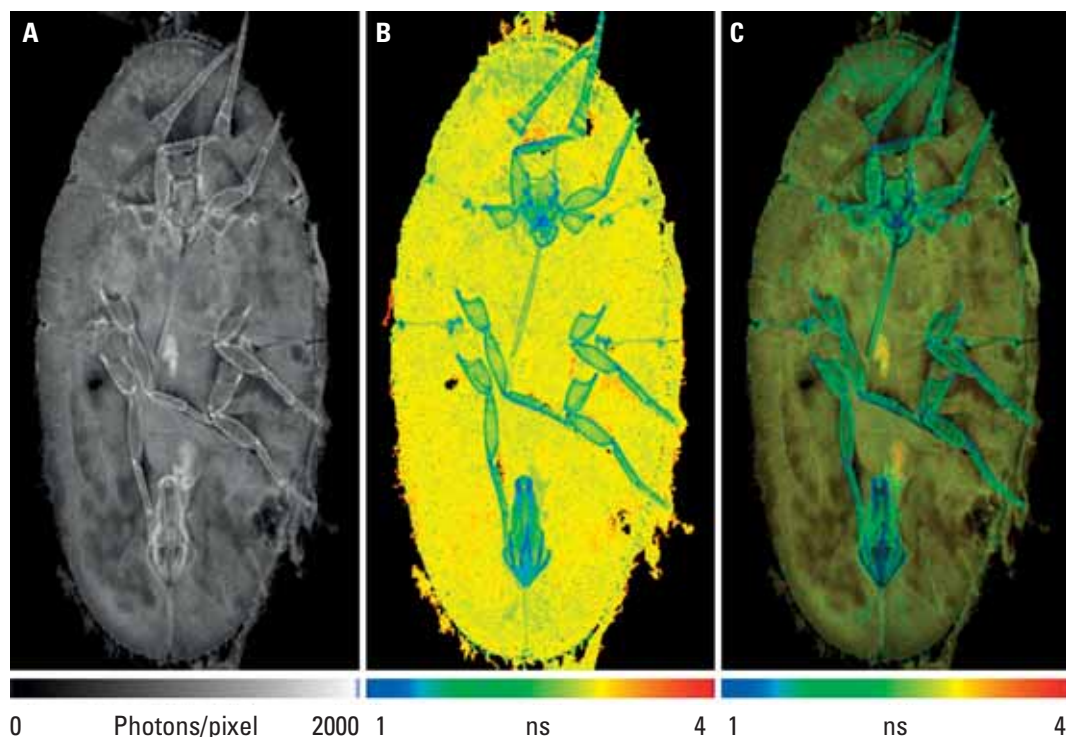


**Fig. 1** Autofluorescence image of scale insect (ventral view). Intensity image (A), lifetime map (B, background cropped) and intensity modulated lifetime image (C). The lifetime map shows the spatial resolution of at least three different color-coded lifetimes. The length is 1.5 mm, the thickness of the section represents 1.3  $\mu$ m. Scan format 280 x 512, objective lens 10x NA 0.4, excitation with 470 nm, detection of emission from 478 nm to 703 nm (sample courtesy of Kees Jalink, NCI, Amsterdam, Netherlands).

**Fig. 2** FLIM z-stack of antenna of scale insect. 40 z-slices of about 1  $\mu\text{m}$  depth have been recorded using a 40x NA 1.25 lens (A). A maximum projection of the organ shows the antenna and some chitinized hairs (B). Maximum projection was done using external software. The Field-Of-View is 388 x 151  $\mu\text{m}$ .

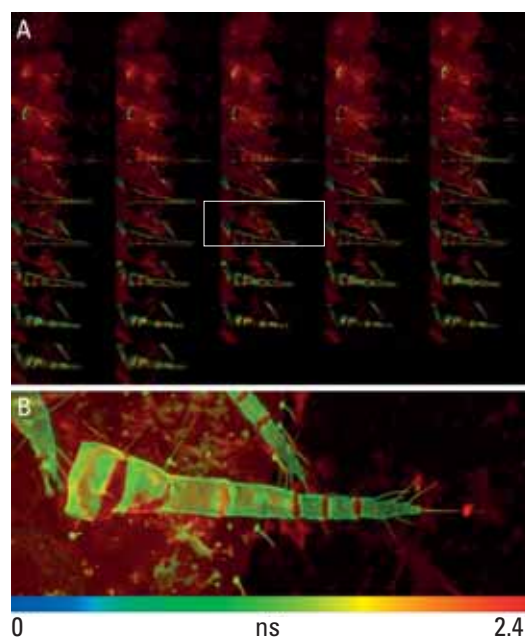


**Fig. 3** 3D rendering of antenna using the image stack presented in Fig. 2. The chitinized structures appear in isosurface rendering with shading (green) overlaid by a volume rendering of the surrounding tissue. (Visualization was done using external software).

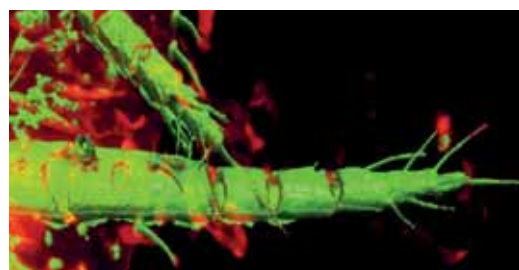
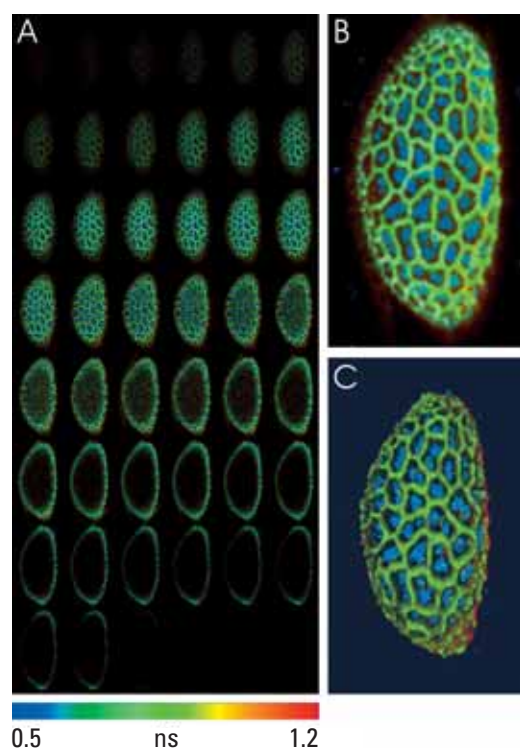


**Fig. 4** Microspore (pollen grain) from *Lilium* sp. (lily flower). Autofluorescence excitable with 470 nm reveals two structurally distinct fluorescent species in the outer layers of the tube cell. 45 z-slices taken recorded with a 20 x NA0.7 lens detecting emission from 482 nm to 744 nm (A), maximum projection using external software (B) and 3D isosurface rendering using external software (C). The longitudinal extension of the spore is 130  $\mu\text{m}$ .



### In depth – 3D FLIM stacks

Taking a closer look at the autofluorescence image (Fig. 1) we recognize that the antennae, for example, have blue regions outside and green regions inside. So, does the green region represent a distinct species or is it rather an (optical) mixture of chitin fluorescence (encoded in blue) and the surrounding tissue (encoded in yellow)? To address this question we can use a higher NA objective on a smaller region. We also have to take into account the z-extension of the image. To better visualize the interior of the structure we can record a FLIM z-stack (Fig. 2). It turns out that the smaller lifetime is caused by chitin, since the interior of the antenna has the same lifetime as the surrounding tissue revealed by a middle section (Fig. 2 A, white box). Thick structures can now be viewed in extended focus using a maximum projection of the z-stack (Fig. 2, B). An even larger appreciation of the 3D topology is facilitated by an isosurface rendering (Fig. 3). Note, the joints are free of chitin, which is clearly visible in the FLIM data. Important taxonomic features become visible, such as the hair-like setae scattered across all body segments. They clearly also contain a chitin species.

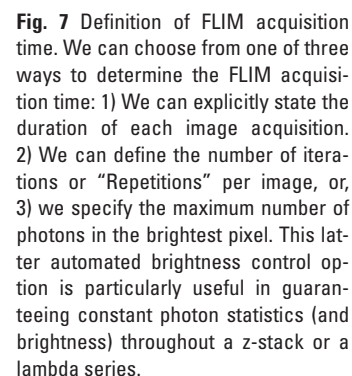
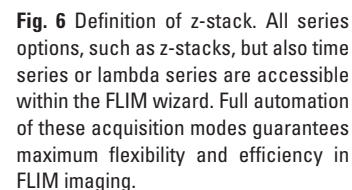
### Multi-color autofluorescence

Fluorescence imaging in plants is often somewhat impeded by the presence of a multitude of fluorescent species, such as chlorophyll and several cell wall constituents as well as a multitude of endogenous pigments. Here we make use of these intrinsic autofluorophores to lend contrast to otherwise poorly distinguishable structures. We recorded a z-stack of a pollen grain (microspore) taken from a lily flower (Fig. 4). The anthers of the pollen grains have a yellow-orange color visible by eye as well as in transmission light (not shown). Possible candidates for such yellow fluorochromes in the plant kingdom are, for example, carotinoids. We obtained lifetimes ranging from 0.5 ns to 1.2 ns. Two main structural features were clearly contrasted by lifetime. In green we recognize the net-like outer layer of the (putative) tube cell, which surrounds the core rendered in blue (0.5 ns). Z-sectioning reveals that the core is not filled with the short lifetime species, but it rather forms a thin inner layer around the tube cell (Fig. 4 A). Extended focus (Fig. 4 B) and 3D visualization (Fig. 4 C) help to clarify the relative topology of both layers to one another.





In autofluorescence imaging the fluorophores are generally not known *ab initio*. Thus, the first step often is to determine the optimal excitation wavelength. In the SMD system used three pulsed lasers were available: 405, 470 and 640 nm. It turned out that 470 nm excites different species. It is very helpful to use the “RunFLIMTest” option in Step 2 of the FLIM wizard in LAS AF to generate a FLIM preview image Fig. 5, ①. This image is displayed in SymPhoTime. It is based on estimating the fluorescence lifetime from the average start-stop times (i.e., half-maximal decay) of the fluorescence decay histograms. Here, no curve-fitting is involved and the FLIM image is displayed in real-time. The color-coded image reveals the presence of at least two distinct species in the hyphae. We set a suitable range for the z-Galvonometer stage to capture about half the depth of the pollen grain with e.g. 45 sections Fig. 6, ②. Choices of detectors can be made in this step as well. Here we are using internal detectors to record emission light from 482 – 744 nm. We switch to Step 3 (Fig. 5, ③) and determine the recording time. In this case we used the automated brightness control feature (Fig. 7, ④) to ensure manageable photon statistics throughout the stack. Now, it’s simply about pressing “RunFLIM” (Fig. 8, ⑤) and we are



done. In SymPhoTime we can display the lifetime distribution (Fig. 9, ⑥). Both by its two maxima as well as the coloring of the FLIM images we can clearly distinguish two different species. To maximize contrast we can set two cursors in the lifetime distribution viewer (Fig. 9, ⑦) or type in

a number (Fig. 9, ⑧). We do the latter and set the upper and lower bounds to 0.5 ns and 1.2 ns, respectively. Clicking on ⑨ (Fig. 9) applies these settings to all images which belong to the stack. For publication purposes we can export the images in common file formats (Fig. 9, ⑩).

**Fig. 8** Step 3 of FLIM wizard. Set up of FLIM series and duration of FLIM acquisition

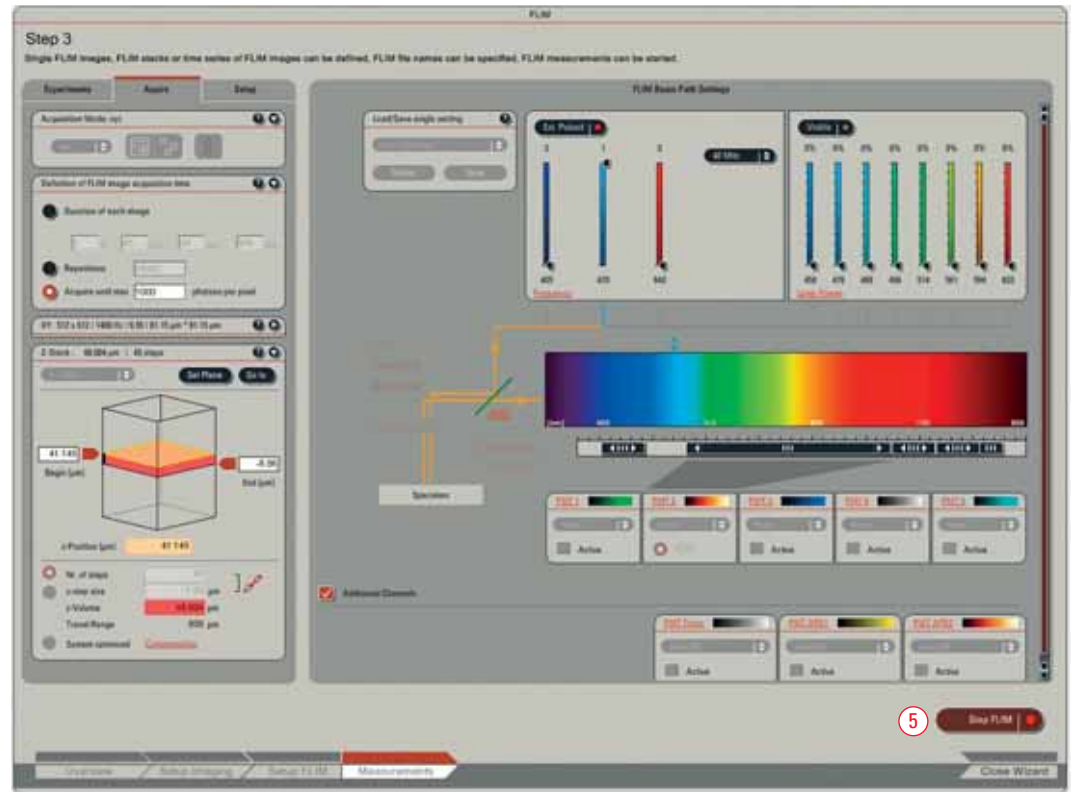
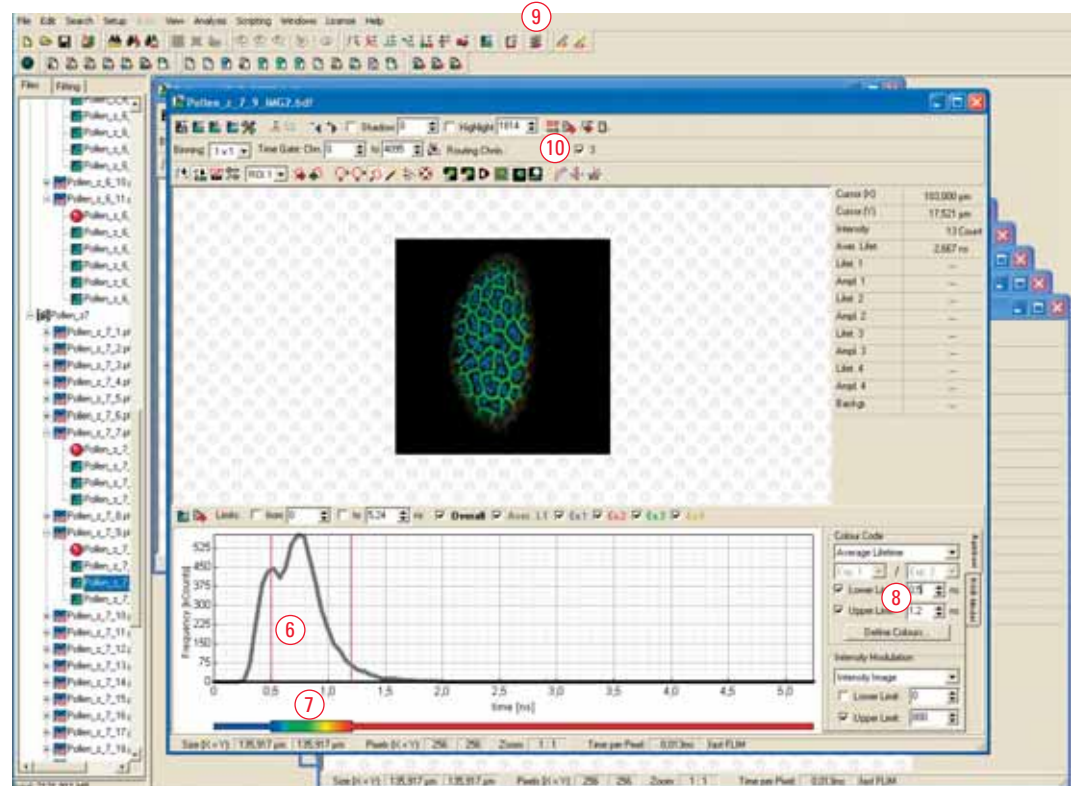


**Fig 9** Distribution of average lifetimes in SymPhoTime software. The user can rescale the look-up table for lifetimes and apply these settings to multiple images in one stack.



### Functional interactions

So far, we mostly used FLIM as a label-free contrasting method, which is a good tool to study the 3D topology of a sample or distinguish different structures. But now that we have got all players on stage we can take the next step and analyze the fluorophore composition in an unlabeled sample in more detail. We remain in the plant kingdom and study the interactions between the host tissue and a pathogenic fungus inside a tomato fruit.

We record an overview image using 405 nm excitation. Invading fungal hyphae, chromoplasts, and some (putative) parenchymal tissue are clearly visible. Using a broad detection range from 413 – 766 nm a poorly contrasted intensity image is obtained (Fig. 10 A). The corresponding FLIM image dramatically highlights the wide range of lifetime species present in this sample (Fig. 10 B). Very prominently chromoplasts (colored in blue) display a lifetime around 0.5 ns. The main constituent contributing to this short lifetime are possibly carotenoids (compare spore example above). The invading hyphae are contrasted by their cell walls showing rather homogenous lifetimes. The autofluorescence of cell walls appears at around 0.9 ns, clearly shown in Fig. 10 B. The central structure in Fig. 10 B represents a part of parenchymal tissue left during the preparation. It has a lifetime which is distinct from the other two structures in the image. Evidently, all structures are intricately interwoven and the sample contains a wide range of different lifetimes. As in most biological samples autofluorescence is given rise to by a multitude of biochemical species. How can we disentangle this inherent complexity?

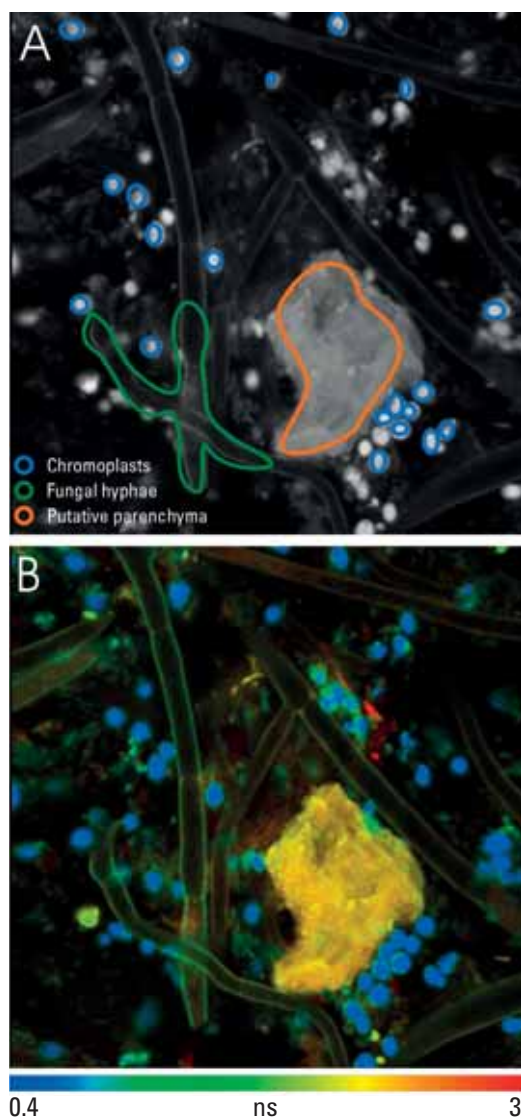


**Fig. 10** Hyphae of pathogenic fungus invading host tissue of tomato fruit. The fungus had afflicted the joint at the base of the fruit leading to subcutaneous lesions. The skin was gently peeled off and its inner face was studied by FLIM using 405 nm excitation. Intensity image (A) showing ROIs used for quantification and FLIM image (B). Functionally different structures like chromoplasts, hyphae and parenchyma display clearly distinguishable fluorescence lifetimes as visualized in false-colors (blue, green and yellow, respectively).

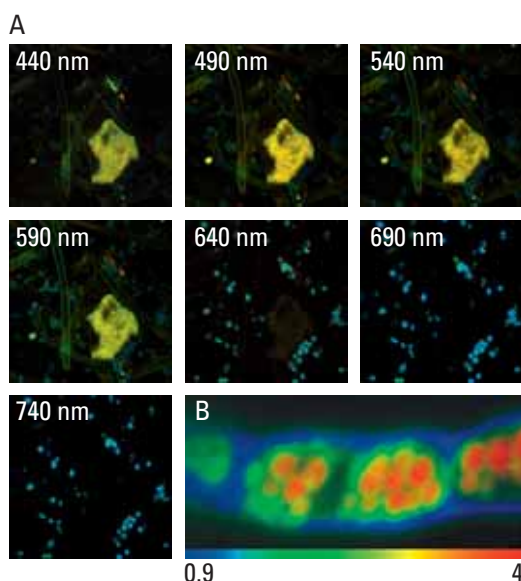


**Fig. 11** Spectrally resolved FLIM image series (A) and single cell of fungal hypha (B). A FLIM lambda stack was recorded in 7 contiguous wavelength bands at 50 nm width each from 415 nm to 755 nm. The central wavelength is given in white. Different components light up selectively in different spectral bands. Some show strong spectral overlap between, for example, fungus and parenchyma, underlining the inherent complexity. (B) reveals subcellular detail inside the hypha contrasted by FLIM.



**Fig. 12** Normalized intensity spectra (=Vis-spectra) of chromoplasts (blue line), fungal hyphae (green) and parenchymal tissue (orange). Colors correspond to ROIs shown in Fig. 7 A. Strong overlap makes it impossible to separate all autofluorescence components spectrally only.

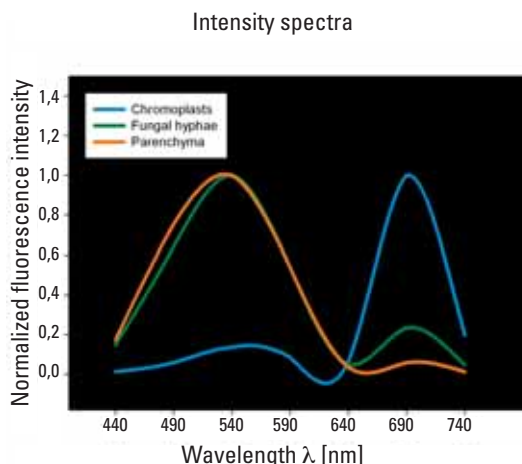
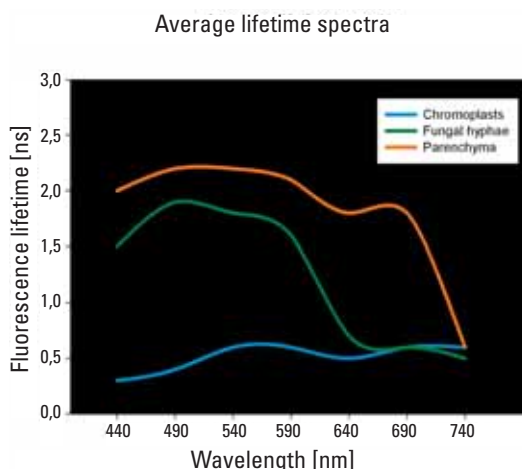


**Fig. 13** Fluorescence lifetime spectra of chromoplasts (blue line), fungal hyphae (green) and parenchymal tissue (orange). For each region of interest mean lifetimes were determined and plotted over wavelength. Colors correspond to ROIs shown in Fig. 7 A. Each lifetime component stays rather constant within the spectral range defined by its underlying fluorescent species (plateau in each curve). Outside this constant range contamination with other species leads to a distortion of detected lifetimes.



### Spectral separation

As a first approximation we can try to spectrally separate the different fluorescence components. To do so, we can record a FLIM lambda series using internal SP detectors (Fig. 11 A). The autofluorescence of both parenchyma and hyphae show a strong overlap, as evident from images ranging 440 – 590 nm (central wavelength). The fluorescence from chromoplasts still appears to be contaminated at 640 nm and above. We can make the interpretation more quantitative by plotting fluorescence intensities against wavelength (Fig. 12). To this end mean intensities are read from the intensity image. For each different structure regions of interest (ROI) were selected as shown in Fig. 10 A (for details please refer to Application Letter 35, FLIM-FRET). The lifetime distribution histogram contains all photons belonging to a given ROI. So its integral is equivalent to the intensity in this region. Thus, for each ROI and each wavelength band the lifetime distribution is exported in ASCII format from SymPhoTime and the photon numbers were

summed up resulting in 7 detection bands x 3 ROIs = 21 intensity values. These were plotted over the corresponding central wavelength to result in the intensity spectra shown in Fig. 12. The spectral overlap between hyphae (green) and parenchyma (orange) becomes very obvious here, particularly from 440 – 590 nm. Some spectral overlap above 640 nm also prevails between fungal hyphae (green) and chromoplasts (blue). So, a purely spectral separation of all components as in traditional fluorescence microscopy is impossible. This is one of the main reasons why autofluorescence is dreaded by many microscopists.

### Lifetime spectra

We are, however, in the position to make use of lifetime information as well, we even have the data already available. The lifetime histograms which were exported before can be interpreted by their mean or median lifetime. Here, the most frequent lifetime was determined as the mean lifetime and confirmed graphically as the (single) peak in the histogram of lifetime distributions as displayed in SymPhoTime. So, again we obtain 7 values per ROI which can be plotted as a function of wavelength (Fig. 13). The structure of these fluorescence lifetime spectra differs from the intensity spectra in that there are no clearly defined peaks. Rather, the lifetime remains close to a maximal value over a much larger wavelength range. While this confirms the robustness of fluorescence lifetimes we still need to use additional information when it comes to separating all the species. The next paragraph will outline a strategy how to do this.



### Fluorescence lifetime fingerprinting

We still have not made full use of the data which we obtained so far. To produce Fig. 12 and Fig. 13 we aggregated the data either to obtain the integral of all photons (as for the intensity spectra) or we used the mean lifetime to produce Fig. 13. What we really have here, however, are photon counts as a function of both wavelength and lifetime. Consequently, we could use the lifetime distribution data to generate a table (or matrix, mathematically speaking) containing these function values. A convenient way to visualize such a data set is a two-dimensional contour plot. This was realized in Fig. 14. Here, photon counts are color-coded (i.e. dependent variable) and x- and y-coordinates represent wavelength (i.e. different images in the lambda series) and fluorescence lifetimes, respectively. For each ROI seven lifetime distributions were exported (corresponding to each wavelength band) and hence, for each ROI a 7 (wavelengths) x 103 (lifetimes) matrix was obtained. All three ROIs were summed to underline their relative positions in the lifetime-wavelength plane. Each sum of lifetime distributions likewise stands for one column in this diagram. The sum along the y-axis would result in the total intensity spectrum. All three structures, chromoplasts, hyphae and parenchyma, can be separated in two-dimensional parameter space. The spectra are seen in Fig. 14, A-C. In this way it is possible to identify fluorescence species corresponding to subsets of this data space. Each peak constitutes a fingerprint reminiscent of protein bands in 2D PAGE analysis. With both fluorescence lifetime and spectral information combined we have a tool at our disposal which reveals much more about the origin of fluorescence in complex mixtures than previously possible. Such multidimensional data sets are now generated using the SMD series in a straightforward way. The data is just waiting to be mined.

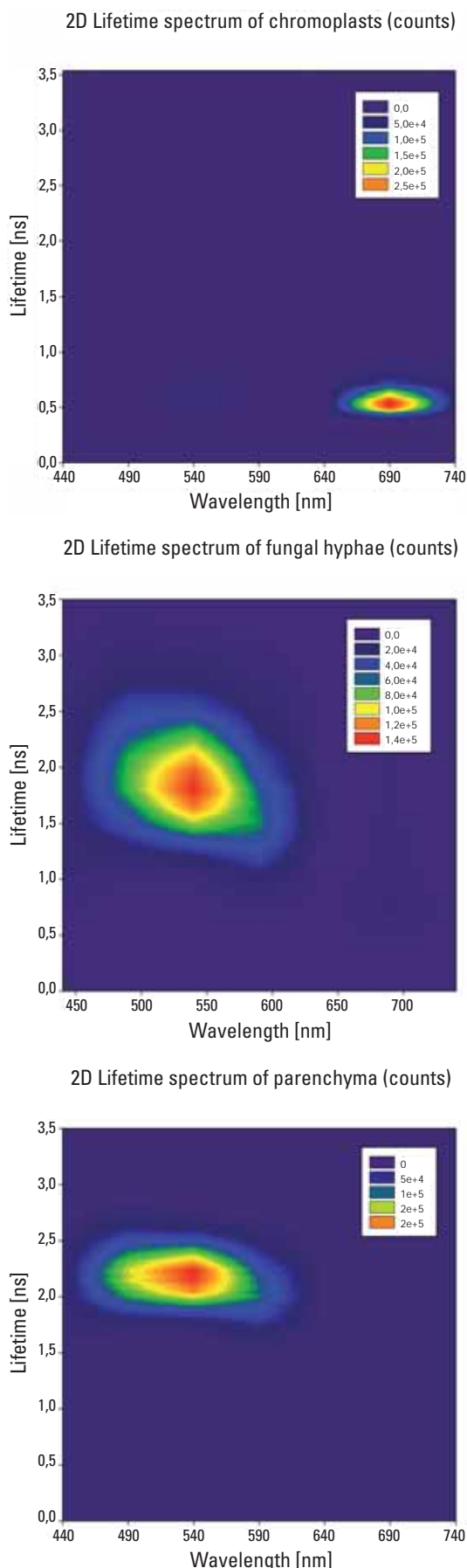


**Fig. 14** 2D lifetime spectra of chromoplasts (A), fungal hyphae (B) and parenchyma (C), respectively. For each type of structure seven lifetime distributions were exported (corresponding to each wavelength band). Lifetimes were scaled from 0 to 3.5 ns and subdivided into 103 discrete values. The resulting matrices were visualized individually using external software. Photon counts are color-coded. Three distinct peaks are discernible corresponding to each structure found in the sample.

### **Autofluorescence – from curse to blessing?**

In this application letter we roughly outlined the potential of autofluorescence imaging in conjunction with FLIM. This is by no means intended to replace extrinsic labeling with conventional fluorescent dyes. Those have evolved towards a much larger quantum yield and molecular brightness while usually having a more narrow emission spectrum than most autofluorescence species. Nevertheless, this application letter intends to demonstrate that autofluorescence can complement fluorescent labels in FLIM imaging as it is much easier to separate fluorescent species using lifetimes than spectral detection alone. Moreover, in some cases, it can even be used to identify multiple functional substructures.

### **Potential clinical outlook**

FLIM makes elegant use of autofluorescence, so it can also serve as label-free contrast in tissue. As reported by Galletly et al. (1) FLIM is capable of providing contrast to fresh biopsy samples where it can help to distinguish precancerous neoplasias from neighboring tissue. Still, research has to be done exploring the parameters and molecular species which define these differences. The utility of FLIM in this field has been demonstrated, so it may develop into a more common tool for clinical research in the future.

### **Information-rich imaging**

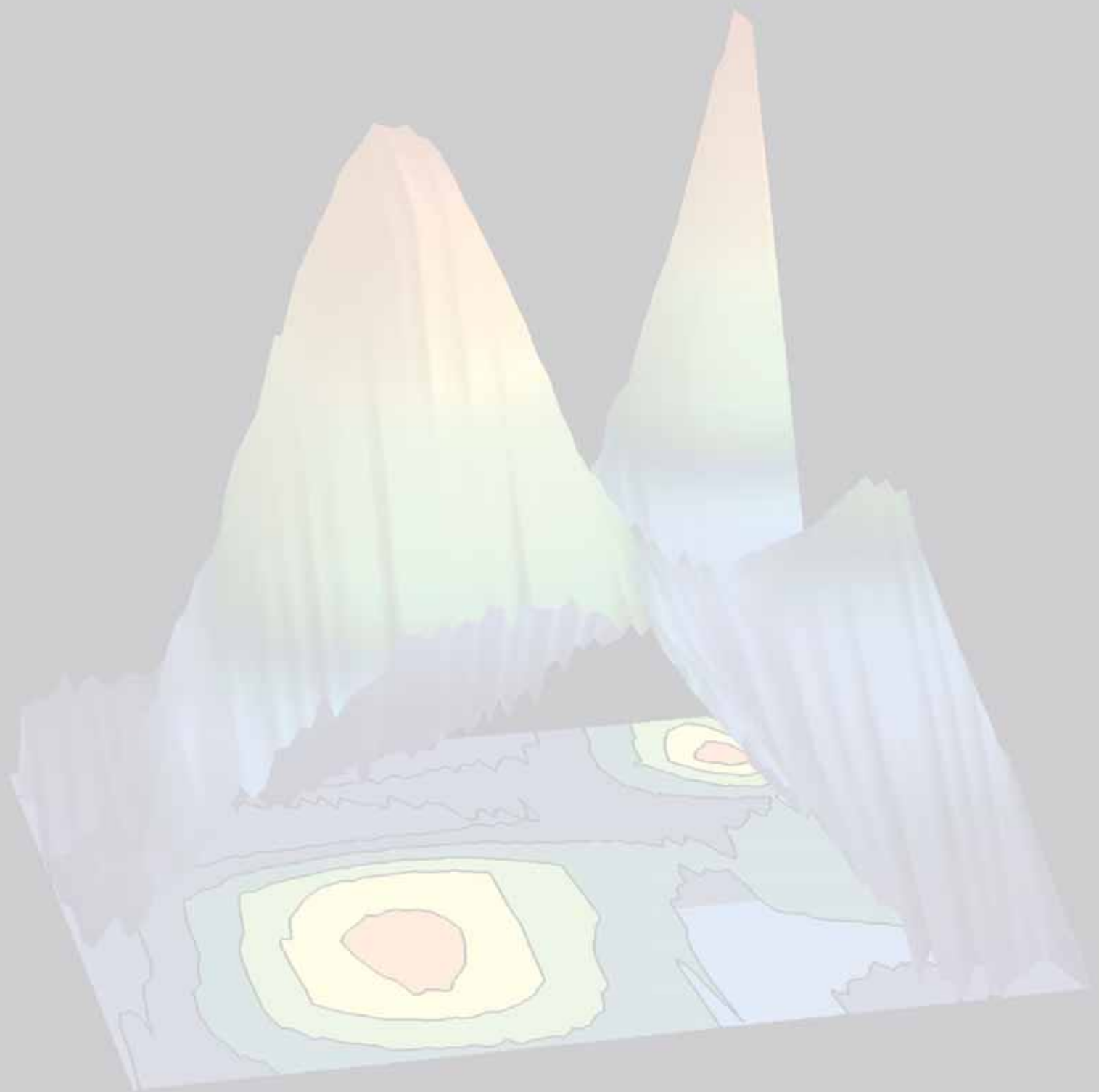
2D lifetime-emission spectra allow researchers to dissect the overlapping contributions to overall fluorescence along the dimensions of both lifetime as well as wavelength. Each autofluorescent species can be identified by its position and intensity in this parameter space like a fingerprint – with much less overlap than using either wavelength or lifetime alone. By working out the fingerprints of a larger number of autofluorescent species researchers have the opportunity to obtain much more informative images: Every region of interest contains the information which was formerly only available by using a larger “zoo” of spectroscopic devices. Therefore, it is now possible to measure many biophysical parameters in the same sample in a spatially resolved fashion – in a comparatively short time.

### **References**

1. Galletly NP, McGinty J, Dunsby C, Teixeira F, Requejo-Isidro J, Munro I, Elson DS, Neil MA, Chu AC, French PM, Stamp GW. “Fluorescence lifetime imaging distinguishes basal cell carcinoma from surrounding uninvolved skin.” *Br J Dermatol*. 159:152-61 (2008)

### **Acknowledgement**

We acknowledge proofreading by  
Dr. Marcelle König, PicoQuant GmbH, Germany





# "With the user, for the user"

## Leica Microsystems

Leica Microsystems operates globally in four divisions, where we rank with the market leaders.

### • Life Science Division

The Leica Microsystems Life Science Division supports the imaging needs of the scientific community with advanced innovation and technical expertise for the visualization, measurement, and analysis of microstructures. Our strong focus on understanding scientific applications puts Leica Microsystems' customers at the leading edge of science.

### • Industry Division

The Leica Microsystems Industry Division's focus is to support customers' pursuit of the highest quality end result. Leica Microsystems provide the best and most innovative imaging systems to see, measure, and analyze the microstructures in routine and research industrial applications, materials science, quality control, forensic science investigation, and educational applications.

### • Biosystems Division

The Leica Microsystems Biosystems Division brings histopathology labs and researchers the highest-quality, most comprehensive product range. From patient to pathologist, the range includes the ideal product for each histology step and high-productivity workflow solutions for the entire lab. With complete histology systems featuring innovative automation and Novocastra™ reagents, Leica Microsystems creates better patient care through rapid turnaround, diagnostic confidence, and close customer collaboration.

### • Surgical Division

The Leica Microsystems Surgical Division's focus is to partner with and support surgeons and their care of patients with the highest-quality, most innovative surgical microscope technology today and into the future.

The statement by Ernst Leitz in 1907, "with the user, for the user," describes the fruitful collaboration with end users and driving force of innovation at Leica Microsystems. We have developed five brand values to live up to this tradition: Pioneering, High-end Quality, Team Spirit, Dedication to Science, and Continuous Improvement. For us, living up to these values means: **Living up to Life.**

### Active worldwide

Australia:	North Ryde	Tel. +61 2 8870 3500	Fax +61 2 9878 1055
Austria:	Vienna	Tel. +43 1 486 80 50 0	Fax +43 1 486 80 50 30
Belgium:	Groot Bijgaarden	Tel. +32 2 790 98 50	Fax +32 2 790 98 68
Canada:	Richmond Hill/Ontario	Tel. +1 905 762 2000	Fax +1 905 762 8937
Denmark:	Herlev	Tel. +45 4454 0101	Fax +45 4454 0111
France:	Nanterre Cedex	Tel. +33 811 000 664	Fax +33 1 56 05 23 23
Germany:	Wetzlar	Tel. +49 64 41 29 40 00	Fax +49 64 41 29 41 55
Italy:	Milan	Tel. +39 02 574 861	Fax +39 02 574 03392
Japan:	Tokyo	Tel. +81 3 5421 2800	Fax +81 3 5421 2896
Korea:	Seoul	Tel. +82 2 514 65 43	Fax +82 2 514 65 48
Netherlands:	Rijswijk	Tel. +31 70 4132 100	Fax +31 70 4132 109
People's Rep. of China:	Hong Kong	Tel. +852 2564 6699	Fax +852 2564 4163
Portugal:	Lisbon	Tel. +351 21 388 9112	Fax +351 21 385 4668
Singapore		Tel. +65 6779 7823	Fax +65 6773 0628
Spain:	Barcelona	Tel. +34 93 494 95 30	Fax +34 93 494 95 32
Sweden:	Kista	Tel. +46 8 625 45 45	Fax +46 8 625 45 10
Switzerland:	Heerbrugg	Tel. +41 71 726 34 34	Fax +41 71 726 34 44
United Kingdom:	Milton Keynes	Tel. +44 1908 246 246	Fax +44 1908 609 992
USA:	Bannockburn/Illinois	Tel. +1 847 405 0123	Fax +1 847 405 0164

and representatives in more than 100 countries